Inorganic Chemistry Communications xxx (xxxx) 110630

Contents lists available at ScienceDirect

Inorganic Chemistry Communications

journal homepage: www.elsevier.com/locate/inoche

Short communication

Application of zinc carbide nanosheet as a promising material for 5-fluorouracil drug delivery

Mustafa M. Kadhim [a, *], Ahmed Mahdi Rheima [b], Fatin Fadhel Mohammed Al-Kazazz [b], Ali Majdi [c], Omar Ammar Hashim [d], Firas Mohamed Dashoor Al-Jaafari [e], Du'a Abduladheem Umran [f], Mohaned Adel [g], Safa K. Hachim [h, i], Doaa Talib Zaidan [j]

[a] Department of Dentistry, Kut University College, Kut, Wasit 52001, Iraq
[b] Department of Chemistry, College of Science, Mustansiriyah University, Baghdad, Iraq
[c] Department of Building and Construction Techniques Engineering, Al- Mustaqbal University College, 51001 Hilla, Iraq
[d] College of Pharmacy, The University of Mashreq, 10021 Baghdad, Iraq
[e] Department of Physics, College of Science, Wasit University, Al Kut 52001, Iraq
[f] Department of Pharmacy, Mazaya University College, Iraq
[g] Pharmacy College, Al-Farahidi University, Baghdad 10022, Iraq
[h] College of Technical Engineering, The Islamic University, Najaf, Iraq
[i] Medical Laboratory Techniques Department, Al-Turath University College, Baghdad, Iraq
[j] Department of Laser and Optical Electronics Engineering, Kut University College, Al Kut, Wasit, Iraq

ARTICLE INFO

Keywords:
Zinc carbide nanosheet
Density functional theory
Electronic properties
5-fluorouracil

ABSTRACT

One of the primary causes of human death is cancer whose treatment using a theranostics strategy is of considerable significance. Density functional theory (DFT) computations were undertaken for scrutinizing the delivery of the anti-cancer drug 5-fluorouracil (5FU) using a zinc carbide nanosheet (ZnC_3NS). The topological, electronic, adsorption energies, charge transfer and the drug release of 5FU@ZnC_3NS were calculated. The obtained adsorption energy for 5FU@ZnC_3NS was −1.45 eV. The charge distributions, electronic properties, and the frontier orbitals were investigated for analyzing the interaction properties of 5FU with the ZnC3NS. Additionally, the natural bond orbital (NBO) analysis showed the occurrence of a charge transfer from 5FU to the ZnC_3NS. In the complex of 5FU@ZnC_3NS, the solvent effects reduced the binding energy of 5FU. The findings demonstrated the possibility of protonating 5FU in the tumor tissues, which facilitated the release of 5FU from the ZnC_3NS. This was the first study which demonstrated the capability of ZnC_3NS in delivering 5FU.

1. Introduction

In the world, one of the primary causes of human death is cancer [1, 2] whose effective treatment with minimum side effects is considered to be of paramount importance. Early and correct diagnosis of cancer can be conducive to reducing the death rate of cancer [3–6]. One of the common methods which is used for cancer treatment is chemotherapy. However, injuring healthy tissues because of its poor selectivity is a major drawback to this method [7]. In recent years, cancer continuous to be one of the fast-growing diseases globally and its effective treatment has become considerably significant [8]. One of the hot topics debated by different researchers and scientists is reducing the side effects of cancer treatment on patients [9]. These days, researchers are considering developing effective anti-cancer drug delivery systems (DDSs) to treat cancer effectively. Accurate cancerous cell targeting and protection of drugs from damages can enhance the therapeutic value of drugs and reduce their toxicity [10]. In appropriate DDSs, drugs have selective distribution in cancerous cells and there is uptake to specific cell types. The side effects of proprietary nanocarriers designed for specific drugs are much less than other systems. [11,12]. The side effects are reduced when drugs attack target cells selectively [13–23].

The drug fluorouracil (5FU) is extensively used in liver, colorectal, pancreatic, breast, gastric cancers chemotherapy, as well as squamous cell carcinomas of the neck and head. Despite its widespread applications, 5FU has serious side effects such as neurotoxicity, myelotoxicity, and cardiotoxicity [24]. Therefore, researchers have developed numerous techniques for improving its bioavailability for reducing its side effects [25]. In addition, DDSs have enjoyed considerable attention be-

* *
E-mail address: Mustafa_kut88@yahoo.com (M.M. Kadhim).

https://doi.org/10.1016/j.inoche.2023.110630
Received 17 September 2022; Received in revised form 9 March 2023; Accepted 12 March 2023
1387-7003/

Back to online

cause of their capability of effective controlling of drug release into a diseased tissue, thereby decreasing the toxicity of drugs and increasing their therapeutic efficiency at the same time [26]. Therefore, it is of great importance to explore more effective drug delivery strategies for the 5FU [27,28].

Using nano-materials as drug carriers is an effective method which has been recently considered for minimizing the side effects of drugs and for raising their selectivity. Because of their applications in producing lighter and stronger materials, water decomposition and drug development, nano-materials have enjoyed considerable attention [29–33]. Nano-materials can be defined as materials which have an external dimension that measures 1–100 nm [34–39]. Researchers have investigated nano-materials for drug delivery owing to their great bioavailability [40–46]. Using nano-sheets, which are common nano-materials, as drug delivery vehicles is an effective method for targeting specific cancerous cells [47,48]. One of the well-known nano-materials is graphene (Gr) which has received considerable attention because of its unique properties [49–54]. Recently, two-dimensional graphene-based nano-sheets, such as zinc carbide nano-sheet (ZnC_3NS), aluminum nitride nano-sheet (AlNNS), and boron nitride nano-sheet (BNNS), have enjoyed considerable attention in nanotechnology since they have large band gap, strong light adsorption capability, high mechanical strength, high conductance, high carrier mobility as well as high thermal stability. [55–63]. Therefore, in ZnC_3NS with a compact structure with graphene sheets, two carbon atoms are replaced with zinc atoms to obtain the ZnC_3 monolayer. Understanding the interaction between the ZnC_3NS and 5FU would be interesting.

In this work, the adsorption behavior of the ZnC_3NS towards 5FU was investigated by applying DFT. Moreover, to explore the adsorption behavior of 5FU on the ZnC_3NS, adsorption energies, electrostatic potential (ESP) maps, charge transport, and interaction distances were analyzed. Dipole moment and the ZnC_3NS surface were used to investigate the impact of the solvent polarity.

2. Computational methodology

The Gaussian 03 program was utilized for undertaking all of the calculations [64]. One of the useful tools to characterize inter-molecular interactions is DFT [65]. The geometries were optimized through the Perdewe-Burkee-Ernzerhof (PBE) functional with the basis set 6-31 g (d, p) [66]. Based on the literature, this method yields accurate results [67,68]. The van der Waals interaction for short-range interactions was also investigated. Hence, DFT-D3 (dispersion correction) was employed [69]. The calculations were undertaken in the gas phase under spin-unrestricted manner. In order to confirm the true minima, frequency calculations were undertaken on the optimized structures at the same level of theory. The energy of adsorption of 5FU on the ZnC_3NS was computed as follows:

$$E_{ads} = E_{ZnC_3NS+5-FU} - E_{5-FU} - E_{ZnC_3NS} \quad (1)$$

where E_{ads} is the total energy of adsorption, $E_{(ZnC3NS+\ 5FU)}$ is the energy of 5FU adsorbed on the ZnC_3NS, and $E_{(ZnC3NS)}$ is the energy of the isolated ZnC_3NS. $E_{(5FU)}$ is the energy of a single 5FU molecule [70]. The NBO analysis was performed for scrutinizing the charge transport between 5FU and ZnC_3NS.

3. Results and discussions

3.1. Analysis of the optimized structure of ZnC_3NS

Fig. 1 illustrates in detail the optimized ZnC_3NS structure. The two-dimensional honeycomb lattice of ZnC_3 is composed of carbon ring atoms (the first honeycomb) connected to rings of zinc-carbon atoms (the second honeycomb). The optimized lattice parameter is 5.15 Å with a bond angle of 120°, which is a little higher than the reported

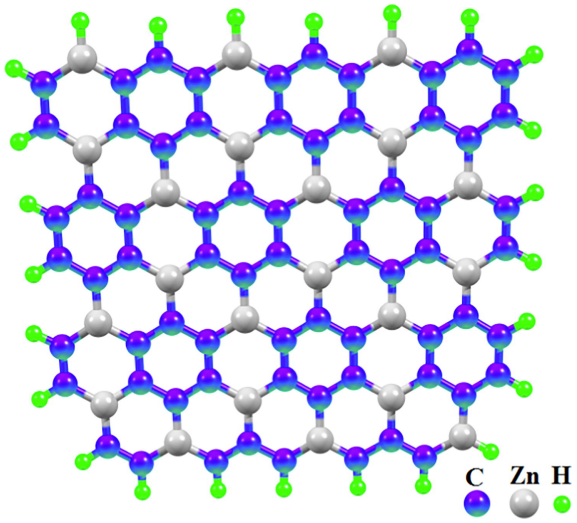

Fig. 1. Upper view optimized structure of the ZnC_3 nanosheet.

value for Gr (4.92 Å) [39]. The distance between two carbon atoms in the first honeycomb is 1.43 Å, which is almost similar to the bond length of Gr (1.41 Å). In the second honeycomb, the distance between two C atoms was 1.44 Å, but the distance between Zn and C atoms was 2.01 Å, which is more than the bond length of Gr. The differences were because of the change in the atomic radius of C and Zn. It The formation energy was approximately −8.90 eV, showing the thermodynamic stability of the ZnC_3NS.

3.2. Optimized geometry and EPS surface of 5FU

There are two types of O, two N atoms and one fluorine in the structure of 5FU (see Fig. 2a). The electrostatic potential (ESP) maps were used for identifying the key structural properties of 5FU necessary for its activity and investigate its interaction with a molecular receptor through recognition in a biological process. Fig. 2b demonstrates the EPS map of the optimized structure of the 5FU molecule. Based on the EPS map of 5FU, O_3 and O_2 atoms were the most favorable sites for nucleophilic attack. These results indicate the most likely interaction area between 5FU anticancer drug and ZnC_3NS is O_3 and O_2 positions.

3.3. 5FU adsorption on the ZnC_3NS surface

5FU was loaded on ZnC_3NS at different sites and the most stable geometries were illustrated in Fig. 3. The drug-loaded complexes of ZnC_3NS were signified as 5FU@ZnC_3NS (5FU-loaded ZnC_3NS). As shown in Fig. 3, the drug interacted via its lone electron pair on oxygen with the Zn atom in the ZnC_3NS. The adsorption energy values were provided in Table 1. The adsorption energy values were used to analyze the potential of 5FU loading on the ZnC_3NS. Complex A_1 had a lower adsorption energy of −0.37 eV compared to complex A_2 with the adsorption energy of −1.45 eV. The complexes A_1 and A_2 were obtained from the interaction of the O_2 as well as O_3 atoms of 5FU with the Zn atom of the ZnC_3NS, respectively. The interaction between 5FU and ZnC_3NS was scrutinized through comparing the bond distances (C–Zn) prior to and following 5FU loading. Following 5FU loading, there was a change in the bond lengths of the isolated 5FU (C = O bond) and ZnC_3NS (Zn–C) (Table 1). These results show an interaction between the drug and nanosheets through Zn–C bond distances 2.01 Å. Upon drug loading, the respective bond lengths were found to be increased. For ZnC_3NS, Zn–C length showed an increment of 0.03 Å. This change in the bond distance suggests that the drug has been absorbed efficiently on the ZnC_3NS surface.

Back to online

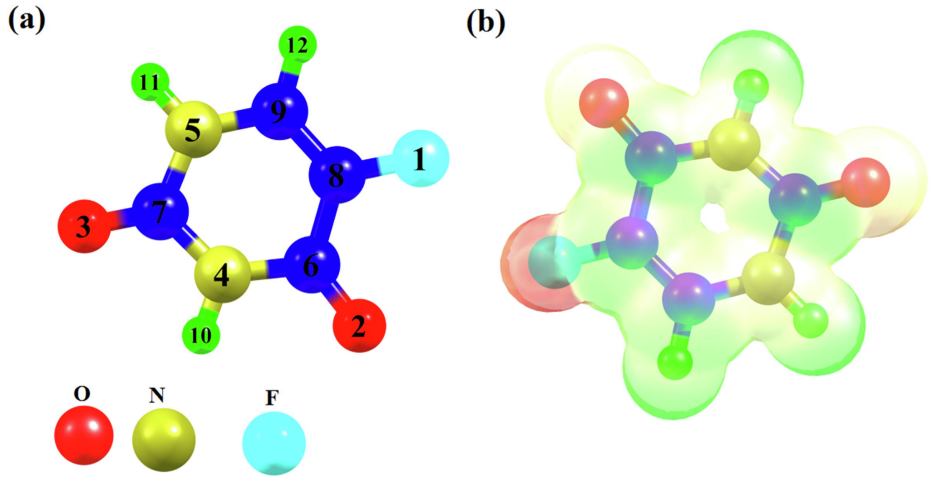

Fig. 2. (a) the optimized structures and (b) the ESP maps of 5FU drug.

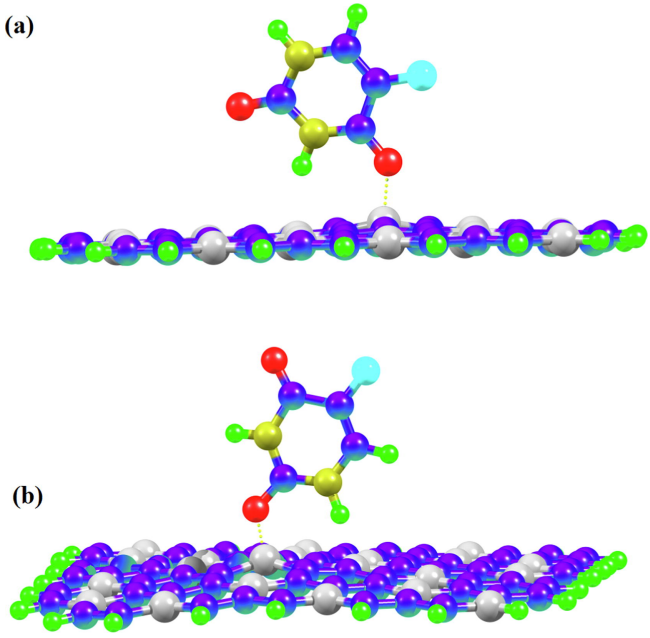

Fig. 3. The optimized structures of different complex of 5FU@ZnC_3NS (a) complex A_1 and (b) complex A_2.

Table 1
Adsorption energies (E_{ads}, eV), and bond lengths before and after drug loading for 5FU adsorbed on ZnC_3NS surface.

System	E_{ads} (eV)	Beforebond lengths (Å)		Afterbond lengths (Å)	
		Zn-C in ZnC_3NS	C=O in 5FU	Zn-C in ZnC_3NS	C=O in 5FU
Complex A_1	−0.37	2.040	1.217	2.030	1.271
Complex A_2	−1.45	2.040	1.216	2.010	1.312

3.4. Analysis of HOMO-LUMO

The frontier molecular orbitals (FMOs) are the reason for the chemical reactivity as well as the kinetic stability of ZnC_3NS for improving the drug delivery performance of 5FU. The HOMO shows the electron-donating ability, whereas the LUMO shows electron-accepting ability. The HOMO-LUMO of ZnC_3NS was demonstrated in Fig. 4 (a, b). The HOMO-LUMO energy gap was used to explain chemical reactivity as well as electron transport. Following the adsorption of 5FU, FMOs were illustrated in Fig. 4 (c, d). In ZnC_3NS, molecular orbital wave functions had an equal distribution throughout the Zn–C or C–C bonds. The HOMO and LUMO of 5FU-adsorbed complexes were localized close to the Zn site, which indicated a charge transport between the 5FU and ZnC_3NS and supported the energies of adsorption [71,72].

3.5. Natural bond orbitals (NBO) analysis

NBO calculations in 5FU-loaded complexes were performed to find the charge transport between the 5FU molecule and the carrier. Apparently, 5FU molecules contained a negative charge and the ZnC_3NS contained a positive charge, which showed that the charge flow was from the 5FU molecule to the ZnC_3NS [45]. However, to gain deeper insights, the second order perturbation energies (E2) were also analyzed and given in Table 2. The results depicted that the most charge transport was from LP (O) → BD* (Zn–C) in complex A_1 with an interaction energy of 3.26 kcal/mol. The lone pair was transported from 5FU to the antibonding orbital (BD*) of the ZnC_3NS.Complex A_2 exhibited a maximum stabilization in LP (O) → LP* (Zn–C) transition with the energy of 6.88 kcal/mol. The findings showed that the electron-donating ability of the lone pair O_3 of 5FU was better than O_2. Hence, complex A_2 facilitated the charge transport and interaction with the 5FU molecule.

3.6. Solvent effect

The self-consistent reaction field method and the conductor-like polarizable continuum model [73,74] were adopted for performing the full geometry optimizations of 5FU, the ZnC_3NS, and complex A_2 for investigating the impact of the water solvent on the interaction of 5FU with the ZnC_3NS as a DDS in the human body [75]. The negative values of solvation energy (ΔE_{solv}) confirmed the stability of the 5FU-ZnC_3NS in the water solvent. ΔE_{solv} was computed as follows [76]:

$$\Delta E_{solu} = E_{solvent} - E_{gas} \quad (2)$$

where $E_{solvent}$ signifies the total energy of the complexes in the solvent and E_{gas} signifies the total energy of the complexes in the gaseous. The ΔE_{solv} value was negative, showing that the solvation of the derived complexes had a major contribution in stabilizing these systems and the ΔE_{solv} of 5FU@ZnC_3NS was −1.64 eV. The negative values of ΔE_{solv} of these complexes indicated that 5FU was soluble in the ZnC_3NS and that the process was spontaneous.

Back to online

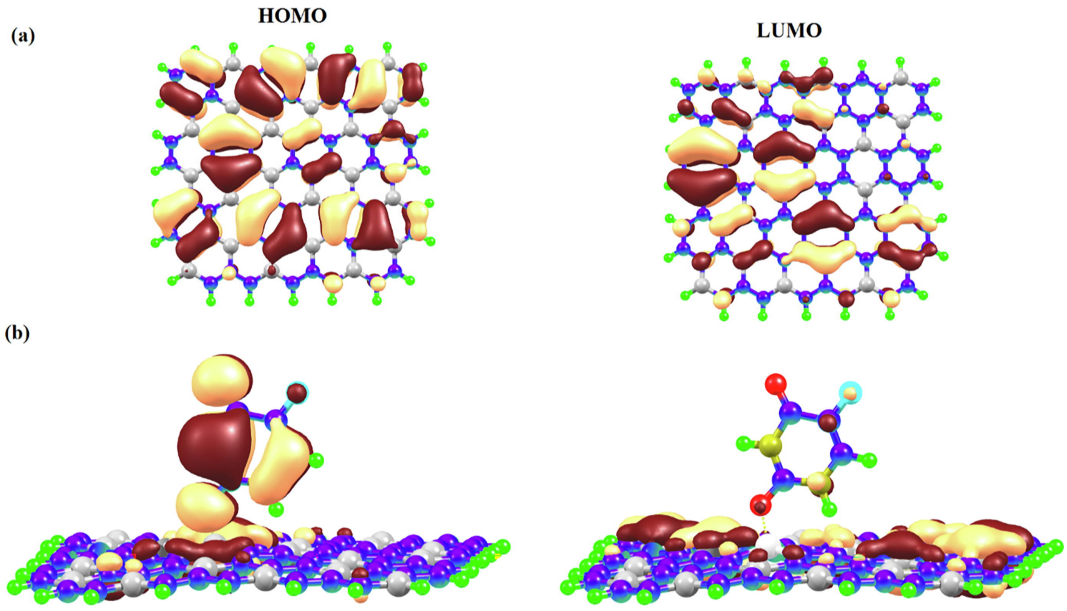

Fig. 4. Frontier molecular orbitals distributions of (a) pristine ZnC3NS and (b) 5FU@ZnC_3NS complex.

Table 2
The NBO analysis of drug loaded complexes on the ZnC_3NS surface.

System	Interaction	E (2) kcal/mol
Complex A_1	LP (O) → BD* (Zn-C)	3.26
Complex A_2	LP (O) → BD* (Zn-C)	6.88

3.7. Recovery time

Another important parameter in drug sensing is the recovery time τ, which is the time taken for the 5FU drug to desorb from the ZnC_3NS. Since complex A_2 had achieved greater energy as well as thermodynamic stability, it was necessary to investigate τ to consider the ZnC_3NS as an effective 5FU nanocarrier. According to M. A. Zaeem and S. Thomas, a short adsorbent τ is favorable for an effective nanocarrier [77]. Hence, τ was computed as follows [78]:

$$\tau = \upsilon^{-1} \exp\left(\frac{-E_{ads}}{k_B T}\right) \quad (3)$$

where ν signifies the frequency (10^{18} s^{-1}), k_B signifies the Boltzmann constant, and T signifies he absolute temperature in Kelvin (298.15 K), τ of 5FU@ZnC_3NS was computed to be 371.02 *ms*, which showed the possibility of utilizing the ZnC_3NS as a DDS.

3.8. The process of 5FU drug release

One of the significant issues for the practical applications of the ZnC3NS as a DDS is the reversibility of the adsorption or desorption of 5FU. Also, one of the key steps in the drug delivery mechanism is the release of 5FU from the nano-carrier in the target cells. A pH-dependent drug release mechanism was reported theoretically by Hazrati et al. [79]. This strategy was used by Shakerzadeh, who demonstrated the promising nature of B_{40} as a nanocarrier for the drug delivery of 5FU despite the fact that the pH of the intracellular environment of a malignant cell was lower compared to the pH of the normal cells [80]. The impact of pH upon complex A_2 was further scrutinized by moving a proton towards the O_3 atom of 5FU. Following the structural optimization, the bond distance between the O_3 (5FU)-Zn (ZnC_3NS) atoms increased dramatically from 1.89 Å to 4.97 Å. Hence, the binding energy of 5FU at ZnC_3NS sharply reduced from −0.51 eV in the slightly acidic medium, reflecting that the drug molecule could be easily detached from this nanosheet when it reached the cancerous cell. 5FU and ZnC_3NS were substantially weakened a single proton approached. Moreover, protonation in the slightly acidic environment of tumor micro-environment could release 5FU easily from the nanosheet, which indicated that possibility of using the ZnC_3NS as a promising nano-carrier for the delivery of 5FU.

4. Conclusion

The capability of ZnC_3NS in delivering 5FU was scrutinized and characterized using DFT calculations. Moreover, the process of interaction between the ZnC_3NS and 5FU was investigated by examining the stability, topologies, and electronic properties including frontier orbitals and NBO analyses. The results showed that ZnC_3NS can be utilized for the delivery of 5FU. The adsorption energy of 5FU on the ZnC_3NS surface was determined to be −0.51 eV in the slightly acidic environment of tumor tissues, showing that this nano-sheet can be used as an effective carrier for 5FU. The recovery time for the strong physisorption of 5FU@ZnC_3NS was calculated to be 371.02 *ms*, indicating the possibility of using the ZnC_3NS as a potential nano-carrier. These findings can provide theoretical and experimental insights into the synthesis and application of the ZnC_3NS.

CRediT authorship contribution statement

Mustafa M. Kadhim : Conceptualization, Methodology, Software, Conceptualization. **Ahmed Mahdi Rheima :** Methodology, Software, Writing – review & editing. **Fatin Fadhel Mohammed Al-Kazazz :** Methodology, Software, Writing – review & editing. **Ali Majdi :** Methodology, Software, Writing – review & editing. **Omar Ammar Hashim :** Methodology, Software, Writing – review & editing. **Firas Mohamed Dashoor Al-Jaafari :** Methodology, Software, Writing – review & editing. **Du'a Abduladheem Umran :** Methodology, Software, Writing – review & editing. **Mohaned Adel :** Methodology, Software, Writing – review & editing. **Safa K. Hachim :** Writing – original draft, Methodology, Software. **Doaa Talib Zaidan :** Writing – original draft, Methodology, Software.

Back to online

Declaration of Competing Interest

The authors declare that they have no known competing financial interests or personal relationships that could have appeared to influence the work reported in this paper.

Data availability

No data was used for the research described in the article.

References

[1] H. Wang, M. Naghavi, C. Allen, R.M. Barber, Z.A. Bhutta, A. Carter, et al., Global, regional, and national life expectancy, all-cause mortality, and cause-specific mortality for 249 causes of death, 1980–2015: a systematic analysis for the Global Burden of Disease Study 2015, Lancet 388 (2016) 1459–1544.

[2] K. Yunus, M. Zuraidah, A. John, A review on the accumulation of heavy metals in coastal sediment of Peninsular Malaysia, Ecofemin. Clim. Change 1 (2020) 21–35.

[3] M. Arruebo, N. Vilaboa, B. Sáez-Gutierrez, J. Lambea, A. Tres, M. Valladares, et al., Assessment of the evolution of cancer treatment therapies, Cancers 3 (2011) 3279–3330.

[4] E. Lee, J. Koo, T. Berger, UVB phototherapy and skin cancer risk: a review of the literature, Int. J. Dermatol. 44 (2005) 355–360.

[5] Y. Feng, F. Li, J. Yan, X. Guo, F. Wang, H. Shi, et al., Pan-cancer analysis and experiments with cell lines reveal that the slightly elevated expression of DLGAP5 is involved in clear cell renal cell carcinoma progression, Life Sci. 287 (2021) 120056.

[6] Z. Zhang, F. Cui, C. Cao, Q. Wang, Q. Zou, Single-cell RNA analysis reveals the potential risk of organ-specific cell types vulnerable to SARS-CoV-2 infections, Comput. Biol. Med. 140 (2022) 105092.

[7] M.M. Gottesman, T. Fojo, S.E. Bates, Multidrug resistance in cancer: role of ATP–dependent transporters, Nat. Rev. Cancer 2 (2002) 48–58.

[8] F. Rehmann, L. Cuffe, O. Mendoza, D. Rai, N. Sweeney, K. Strohfeldt, et al., In-vitro anti-tumor activity studies of bridged and unbridged benzyl-substituted titanocenes, Appl. Organomet. Chem. 19 (2005) 293–300.

[9] S.A. Alavi-Tabari, M.A. Khalilzadeh, H. Karimi-Maleh, D. Zareyee, An amplified platform nanostructure sensor for the analysis of epirubicin in the presence of topotecan as two important chemotherapy drugs for breast cancer therapy, New J. Chem. 42 (2018) 3828–3832.

[10] D.L. Clemens, B.-Y. Lee, M. Xue, C.R. Thomas, H. Meng, D. Ferris, et al., Targeted intracellular delivery of antituberculosis drugs to *Mycobacterium tuberculosis*-infected macrophages via functionalized mesoporous silica nanoparticles, Antimicrob. Agents Chemother. 56 (2012) 2535–2545.

[11] J. Liu, L. Cui, D. Losic, Graphene and graphene oxide as new nanocarriers for drug delivery applications, Acta Biomater. 9 (2013) 9243–9257.

[12] H. Raissi, F. Mollania, Immunosuppressive agent leflunomide: A SWNTs-immobilized dihydroortate dehydrogenase inhibitory effect and computational study of its adsorption properties on zigzag single walled (6, 0) carbon and boron nitride nanotubes as controlled drug delivery devices, Eur. J. Pharm. Sci. 56 (2014) 37–54.

[13] E. Blanco, E.A. Bey, Y. Dong, B.D. Weinberg, D.M. Sutton, D.A. Boothman, et al., β-Lapachone-containing PEG–PLA polymer micelles as novel nanotherapeutics against NQO1-overexpressing tumor cells, J. Control. Release 122 (2007) 365–374.

[14] X. Zheng, P. Blowers, N. Zhang, Application of compound models for estimating rate constants of hydrocarbon thermal cracking reactions: The neopentyl radical β-scission reaction, Mol. Simul. 31 (2005) 615–621.

[15] S. Ai, J. Duan, X. Liu, S. Bock, Y. Tian, Z. Huang, Biological evaluation of a novel doxorubicin– peptide conjugate for targeted delivery to EGF receptor-overexpressing tumor cells, Mol. Pharm. 8 (2011) 375–386.

[16] O.H. Aina, R. Liu, J.L. Sutcliffe, J. Marik, C.-X. Pan, K.S. Lam, From combinatorial chemistry to cancer-targeting peptides, Mol. Pharm. 4 (2007) 631–651.

[17] V.M. Platt, F.C. Szoka Jr, Anticancer therapeutics: targeting macromolecules and nanocarriers to hyaluronan or CD44, a hyaluronan receptor, Mol. Pharm. 5 (2008) 474–486.

[18] W. Tai, R. Shukla, B. Qin, B. Li, K. Cheng, Development of a peptide-drug conjugate for prostate cancer therapy, Mol. Pharm. (2011).

[19] A. Wongmekiat, Y. Tozuka, K. Moribe, T. Oguchi, K. Yamamoto, Preparation of drug nanoparticles by co-grinding with cyclodextrin: formation mechanism and factors affecting nanoparticle formation, Chem. Pharm. Bull. 55 (2007) 359–363.

[20] R. Langer, Drug delivery. Drugs on target, Science (New York, NY) 293 (2001) 58–59.

[21] Y. Peng, C. Shi, Y. Zhu, M. Gu, S. Zhuang, Terahertz spectroscopy in biomedical field: a review on signal-to-noise ratio improvement, PhotoniX 1 (2020) 1–18.

[22] X. Fan, G. Wei, X. Lin, X. Wang, Z. Si, X. Zhang, et al., Reversible switching of interlayer exchange coupling through atomically thin VO2 via electronic state modulation, Matter 2 (2020) 1582–1593.

[23] Q. Zeng, B. Bie, Q. Guo, Y. Yuan, Q. Han, X. Han, et al., Hyperpolarized Xe NMR signal advancement by metal-organic framework entrapment in aqueous solution, Proc. Natl. Acad. Sci. 117 (2020) 17558–17563.

[24] E. Shakerzadeh, Quantum chemical assessment of the adsorption behavior of fluorouracil as an anticancer drug on the B36 nanosheet, J. Mol. Liq. 240 (2017) 682–693.

[25] L. Zhang, Z.-D. Qi, Y.-L. Ye, X.-H. Li, J.-H. Chen, W.-M. Sun, DFT study on the adsorption of 5-fluorouracil on B 40, B 39 M, and M@ B 40 (M = Mg, Al, Si, Mn, Cu, Zn), RSC Adv. 11 (2021) 39508–39517.

[26] A. Yaraghi, O.M. Ozkendir, M. Mirzaei, DFT studies of 5-fluorouracil tautomers on a silicon graphene nanosheet, Superlattice. Microst. 85 (2015) 784–788.

[27] R. Faramarzi, M. Falahati, M. Mirzaei, Interactions of fluorouracil by CNT and BNNT: DFT analyses, Adv. J. Sci. Eng. 1 (2020) 62–66.

[28] A. Kouchaki, O. Gülseren, N. Hadipour, M. Mirzaei, Relaxations of fluorouracil tautomers by decorations of fullerene-like SiCs: DFT studies, Phys. Lett. A 380 (2016) 2160–2166.

[29] R. Rahimi, M. Solimannejad, BC3 graphene-like monolayer as a drug delivery system for nitrosourea anticancer drug: a first-principles perception, Appl. Surf. Sci. 525 (2020) 146577.

[30] S. Sahoo, S. Parveen, J. Panda, The present and future of nanotechnology in human health care, Nanomed. Nanotechnol. Biol. Med. 3 (2007) 20–31.

[31] J. Chen, Z. Zhang, H. Lu, Structure design and properties investigation of Bi2O2Se/graphene van der Waals heterojunction from first-principles study, Surf. Interfaces 33 (2022) 102289.

[32] Y. Liang, J. Li, Y. Xue, T. Tan, Z. Jiang, Y. He, et al., Benzene decomposition by non-thermal plasma: a detailed mechanism study by synchrotron radiation photoionization mass spectrometry and theoretical calculations, J. Hazard. Mater. 420 (2021) 126584.

[33] Y. Wei, C. Chen, C. Tan, L. He, Z. Ren, C. Zhang, et al., High-performance visible to near-infrared broadband Bi2O2Se nanoribbon photodetectors, Adv. Opt. Mater. 10 (2022) 2201396.

[34] D.F. Emerich, C.G. Thanos, Nanotechnology and medicine, Expert Opin. Biol. Ther. 3 (2003) 655–663.

[35] S.K. Sahoo, V. Labhasetwar, Nanotech approaches to drug delivery and imaging, Drug Discov. Today 8 (2003) 1112–1120.

[36] M. Wang, C. Jiang, S. Zhang, X. Song, Y. Tang, H.-M. Cheng, Reversible calcium alloying enables a practical room-temperature rechargeable calcium-ion battery with a high discharge voltage, Nat. Chem. 10 (2018) 667–672.

[37] Z. Wang, L. Dai, J. Yao, T. Guo, D. Hrynsphan, S. Tatsiana, et al., Improvement of Alcaligenes sp. TB performance by Fe-Pd/multi-walled carbon nanotubes: enriched denitrification pathways and accelerated electron transport, Bioresour. Technol. 327 (2021) 124785.

[38] J. Wang, N. Wang, D. Xu, L. Tang, B. Sheng, Flexible humidity sensors composed with electrodes of laser induced graphene and sputtered sensitive films derived from poly (ether-ether-ketone), Sens. Actuators B 375 (2023) 132846.

[39] L. Zhang, Z. Hu, J. Huang, Z. Chen, X. Li, Z. Feng, et al., Experimental and DFT studies of flower-like Ni-doped Mo2C on carbon fiber paper: a highly efficient and robust HER electrocatalyst modulated by Ni (NO3) 2 concentration, J. Adv. Ceram. 11 (2022) 1294–1306.

[40] S.U.D. Shamim, M.H. Miah, M.R. Hossain, M.M. Hasan, M.K. Hossain, M.A. Hossain, et al., Theoretical investigation of emodin conjugated doped B12N12 nanocage by means of DFT, QTAIM and PCM analysis, Physica E 136 (2022) 115027.

[41] M.R. Hossain, M.M. Hasan, H. Rahman, M.S. Rahman, F. Ahmed, T. Ferdous, et al., Adsorption behaviour of metronidazole drug molecule on the surface of hydrogenated graphene, boron nitride and boron carbide nanosheets in gaseous and aqueous medium: a comparative DFT and QTAIM insight, Physica E 126 (2021) 114483.

[42] M. Nishat, M.R. Hossain, M.M. Hasan, M.K. Hossain, M.A. Hossain, F. Ahmed, Interaction of Anagrelide drug molecule on pristine and doped boron nitride nanocages: a DFT, RDG, PCM and QTAIM investigation, J. Biomol. Struct. Dyn. 1–17 (2022).

[43] M.H. Miah, M.R. Hossain, M.S. Islam, T. Ferdous, F. Ahmed, A theoretical study of allopurinol drug sensing by carbon and boron nitride nanostructures: DFT, QTAIM, RDG, NBO and PCM insights, RSC Adv. 11 (2021) 38457–38472.

[44] M.M. Hasan, A.C. Das, M.R. Hossain, M.K. Hossain, M.A. Hossain, B. Neher, et al., The computational quantum mechanical investigation of the functionalized boron nitride nanocage as the smart carriers for favipiravir drug delivery: a DFT and QTAIM analysis, J. Biomol. Struct. Dyn. 1–17 (2021).

[45] H. Chen, Q. Wang, Regulatory mechanisms of lipid biosynthesis in microalgae, Biol. Rev. 96 (2021) 2373–2391.

[46] L. Zhang, J. Huang, Z. Hu, X. Li, T. Ding, X. Hou, et al., Ni (NO3) 2-induced high electrocatalytic hydrogen evolution performance of self-supported fold-like WC coating on carbon fiber paper prepared through molten salt method, Electrochim. Acta 422 (2022) 140553.

[47] E. Duverger, S. Balme, M. Bechelany, P. Miele, F. Picaud, Natural payload delivery of the doxorubicin anticancer drug from boron nitride oxide nanosheets, Appl. Surf. Sci. 475 (2019) 666–675.

[48] U. Srimathi, V. Nagarajan, R. Chandiramouli, Investigation on graphdiyne nanosheet in adsorption of sorafenib and regorafenib drugs: a DFT approach, J. Mol. Liq. 277 (2019) 776–785.

[49] K.S. Novoselov, A.K. Geim, S.V. Morozov, D.-E. Jiang, Y. Zhang, S.V. Dubonos, et al., Electric field effect in atomically thin carbon films, Science 306 (2004) 666–669.

[50] K.S. Novoselov, A.K. Geim, S.V. Morozov, D. Jiang, M.I. Katsnelson, I. Grigorieva, et al., Two-dimensional gas of massless Dirac fermions in graphene, Nature 438 (2005) 197–200.

[51] S.U. Daula Shamim, M.K. Hossain, S.M. Hasan, A. Hossain, F. Ahmed, Ab initio study of N-doped graphene oxide (NDGO) as a promising anode material for Li-ion rechargeable battery, Mol. Simul. 46 (2020) 1135–1145.

[52] X. Zhang, Y. Tang, F. Zhang, C.S. Lee, A novel aluminum–graphite dual-ion

Back to online

battery, Adv. Energy Mater. 6 (2016) 1502588.
[53] Q. Zhang, S. Wang, Y. Liu, M. Wang, R. Chen, Z. Zhu, et al., UiO-66-NH2@ 67 Core-shell MOF as fillers in solid composite electrolytes for high-performance all-solid-state lithium metal batteries, Energy Technol. (2022).
[54] H. Wang, Y. Chen, H. Yu, W. Liu, G. Kuang, L. Mei, et al., A multifunctional artificial interphase with fluorine-doped amorphous carbon layer for ultra-stable Zn anode, Adv. Funct. Mater. 32 (2022) 2205600.
[55] R. Yin, Y. Zhang, W. Zhao, X. Huang, X. Li, L. Qian, Graphene platelets/aluminium nitride metacomposites with double percolation property of thermal and electrical conductivity, J. Eur. Ceram. Soc. 38 (2018) 4701–4706.
[56] M. Vatanparast, Z. Shariatinia, Hexagonal boron nitride nanosheet as novel drug delivery system for anticancer drugs: insights from DFT calculations and molecular dynamics simulations, J. Mol. Graph. Model. 89 (2019) 50–59.
[57] Y. Yong, X. Su, H. Cui, Q. Zhou, Y. Kuang, X. Li, Two-dimensional tetragonal GaN as potential molecule sensors for NO and NO2 detection: a first-principle study, ACS Omega 2 (2017) 8888–8895.
[58] J. Labrousse, K. Belasfar, O. Aziz, A. El Kenz, A. Benyoussef, ZnC3-2D a new material for hydrogen reversible storage predicted by first-principles calculations, Mater. Today Commun. 31 (2022) 103657.
[59] R. Ren, F. Lai, X. Lang, L. Li, C. Yao, K. Cai, Efficient sulfur host based on Sn doping to construct Fe2O3 nanospheres with high active interface structure for lithium-sulfur batteries, Appl. Surf. Sci. 613 (2023) 156003.
[60] H. Yu, Y. Chen, W. Wei, X. Ji, L. Chen, A functional organic zinc-chelate formation with nanoscaled granular structure enabling long-term and dendrite-free Zn anodes, ACS Nano 16 (2022) 9736–9747.
[61] X. Tang, J. Wu, W. Wu, Z. Zhang, W. Zhang, Q. Zhang, et al., Competitive-type pressure-dependent immunosensor for highly sensitive detection of diacetoxyscirpenol in wheat via monoclonal antibody, Anal. Chem. 92 (2020) 3563–3571.
[62] C. Zhao, M. Xi, J. Huo, C. He, L. Fu, Computational design of BC3N2 based single atom catalyst for dramatic activation of inert CO2 and CH4 gasses into CH3COOH with ultralow CH4 dissociation barrier, Chin. Chem. Lett. 34 (2023) 107213.
[63] C. Zhao, M. Xi, J. Huo, C. He, B-Doped 2D-InSe as a bifunctional catalyst for CO 2/CH 4 separation under the regulation of an external electric field, PCCP 23 (2021) 23219–23224.
[64] Gaussian09, R.A. 1, mj frisch, gw trucks, hb schlegel, ge scuseria, ma robb, jr cheeseman, g. Scalmani, v. Barone, b. Mennucci, ga petersson et al., gaussian. Inc., Wallingford CT, vol. 121, 2009, pp. 150–166.
[65] RA, G. 1, mj frisch, gw trucks, hb schlegel, ge scuseria, ma robb, jr cheeseman, g. Scalmani, v. Barone, b. Mennucci, ga petersson et al., gaussian. Inc, Wallingford CT, vol. 121, 2009, pp. 150–166.
[66] J.P. Perdew, K. Burke, M. Ernzerhof, Generalized gradient approximation made simple, Phys. Rev. Lett. 77 (1996) 3865.
[67] M. Ernzerhof, G.E. Scuseria, Assessment of the Perdew–Burke–Ernzerhof exchange-correlation functional, J. Chem. Phys. 110 (1999) 5029–5036.
[68] B. Hammer, L.B. Hansen, J.K. Nørskov, Improved adsorption energetics within density-functional theory using revised Perdew-Burke-Ernzerhof functionals, Phys. Rev. B 59 (1999) 7413.
[69] J. Moellmann, S. Grimme, DFT-D3 study of some molecular crystals, J. Phys. Chem. C 118 (2014) 7615–7621.
[70] H. Rahman, M.R. Hossain, T. Ferdous, The recent advancement of low-dimensional nanostructured materials for drug delivery and drug sensing application: a brief review, J. Mol. Liq. 320 (2020) 114427.
[71] M. Perveen, S. Nazir, A.W. Arshad, M.I. Khan, M. Shamim, K. Ayub, et al., Therapeutic potential of graphitic carbon nitride as a drug delivery system for cisplatin (anticancer drug): a DFT approach, Biophys. Chem. 267 (2020) 106461.
[72] T. Mahboobi, M.R. Zardoost, M.R. Toosi, Phosphorene and Na-, Ca-, and Fe-doped phosphorene as candidates for delivery of mercaptopurine and fluorouracil anticancer drugs, J. Mol. Model. 26 (2020) 1–9.
[73] B. Mennucci, Polarizable continuum model, Wiley Interdiscip. Rev.: Comput. Mol. Sci. 2 (2012) 386–404.
[74] B. Mennucci, J. Tomasi, R. Cammi, J. Cheeseman, M. Frisch, F. Devlin, et al., Polarizable continuum model (PCM) calculations of solvent effects on optical rotations of chiral molecules, Chem. A Eur. J. 106 (2002) 6102–6113.
[75] M.W. Wong, M.J. Frisch, K.B. Wiberg, Solvent effects. 1. The mediation of electrostatic effects by solvents, J. Am. Chem. Soc. 113 (1991) 4776–4782.
[76] M. Chojecki, S. Yourdkhani, D. Rutkowska-Zbik, T. Korona, Stability of endo-and exohedral complexes of all-boron fullerene B40, Comput. Theor. Chem. 1133 (2018) 7–17.
[77] S. Thomas, M. Asle Zaeem, Phosgene gas sensing of Ti2CT2 (T = F−, O−, OH−) MXenes, Adv. Theory Simul. 4 (2021) 2000250.
[78] M. Shahabi, H. Raissi, Investigation of the solvent effect, molecular structure, electronic properties and adsorption mechanism of Tegafur anticancer drug on Graphene nanosheet surface as drug delivery system by molecular dynamics simulation and density functional approach, J. Incl. Phenom. Macrocycl. Chem. 88 (2017) 159–169.
[79] S.A. Aal, DFT study of the therapeutic potential of borospherene and metalloborospherenes as a new drug-delivery system for the 5-fluorouracil anticancer drug, J. Mol. Liq. 119457 (2022).
[80] K. Shayan, A. Nowroozi, Boron nitride nanotubes for delivery of 5-fluorouracil as anticancer drug: a theoretical study, Appl. Surf. Sci. 428 (2018) 500–513.

Back to online

Back to online